https://doi.org/10.5194/acp-2022-180
Preprint. Discussion started: 7 June 2022

Atmospheric Chemistry and Physics Discussions

Retrieving coal mine CH_4 emissions using UAV-based AirCore observations and the GA-IPPF model

Tianqi Shi[1], Zeyu Han[2], Ge Han[3], Xin Ma[1*], Huilin Chen[4,5]*, Truls Andersen[5], Huiqin Mao[6], Cuihong Chen[6], Haowei Zhang[1], Wei Gong[1,7]

[1] State Key Laboratory of Information Engineering in Surveying, Mapping and Remote Sensing, Wuhan University, Luoyu Road No.129, Wuhan 430079, China;
[2]School of Mathematics and Statistics, Wuhan University, Luoyu Road No.129, Wuhan 430079, China;
[3] School of Remote Sensing and Information Engineering, Wuhan University, Luoyu Road No.129, Wuhan 430079, China;
[4]Joint International Research Laboratory of Atmospheric and Earth System Sciences, School of Atmospheric Sciences, Nanjing University, Nanjing, China;
[5]Centre for Isotope Research, Energy and Sustainability Institute Groningen (ESRIG), University of Groningen, Groningen, Netherlands;
[6]Ministry of Ecology and Environment Center for Satellite Application on Ecology and Environment, Beijing, China;
[7] Electronic Information School, Wuhan University, Luoyu Road No.129, Wuhan 430079, China;

Correspondence to: Xin Ma (maxinwhu@whu.edu.cn); Huilin Chen (huilin.chen@rug.nl)

Abstract. The quantification of CH_4 emissions from coal mines has large uncertainty owing to the lack of effective monitoring methods. In this study, we developed a genetic algorithm–interior point penalty function (GA-IPPF) model to calculate the emission rate of large point sources of CH_4 based on concentration sample. This model can provide optimized dispersion parameters and self-calibrate, thus lowering the requirements for auxiliary data accuracy. Meanwhile, we evaluated the influence of multiple parameters on retrieving CH_4-emission rate by the GA-IPPF, including the uncertainty of CH_4 concentration measurements, the number of CH_4 measurements, and the accuracy of meteorological data. Based on the atmospheric CH_4 concentration measurements from a UAV-based AirCore system and the GA-IPPF model, we retrieved the CH_4-emission rates from the Pniówek coal (Silesia coal mining region mine, Poland) ventilation shaft. Results show that, the CH_4 concentrations reconstructed by the model is highly consistent to the measured ones. And the CH_4-emission rates are variable even in a single day, ranging from 639.3±22.8 to 1415.5±68.5 kg/hour on August 18, 2017 and from 342.5±34.8 to 1449.8±57.1 kg/hour on August 21, 2017. The combination of the flexible UAV-based AirCore CH_4 measurements and the robust GA-IPPF model provides an effective means to quantify CH_4 emissions.

1.Introduction

The release of CH_4 into the atmosphere during coal mining is very concerned because it contributes to increased atmospheric concentration of CH_4, one of the most important greenhouse gases and is a waste of resources (Cardoso-Saldana and Allen, 2020; Zhang et al., 2020). However, CH_4 emissions during coal mining are not always stable owing to different collection mode, manufacturing processes, weather fluctuations, as well as terrain effects (Nathan et al., 2015b). Bottom-up inventories could provide us with approximate CH_4-emission rates from strong sources. However, inventory data cannot serve as a reference for proposing new policies to reduce anthropic CH_4 emission because of their low temporal resolution and large uncertainty. The temporal resolution and accuracy of bottom-up inventory are too low to obtain emission information instantly (Pan et al., 2021; Liu et al., 2020). Thus, it's of great need

https://doi.org/10.5194/acp-2022-180
Preprint. Discussion started: 7 June 2022

to develop a high-accuracy retrieval model to obtain emission intensity based on top to down methods. With the development of different measurement technologies for atmospheric CH_4, the CH_4 emission rate has become possible to be quantified.

Greenhouse gases observing satellite and TROPOspheric Monitoring Instrument could obtain the column concentration of CH_4 (XCH_4, ppb) with a spatial resolution of 10 km×10 km and 5 km×7.5 km, respectively. The regional CH_4 flux could be retrieved by assimilating the measured XCH_4 into an atmospheric dispersion model (Tu et al., 2022; Feng et al., 2016). PRISMA hyperspectral imaging satellite and GHGsat could detect increased CH_4 caused by strong emission sources with high spatial resolutions, and the comprehensive CH_4 emission could be quantified by integrated mass enhancement or cross-sectional flux method (Guanter et al., 2021; Varon et al., 2020). However, CH_4 emission during coal mining is not constant even in a short period of time, and the spatial and temporal resolutions of satellites don't allow to repeated quantification of CH_4 emission from coals in the same day (Schneising et al., 2020; Varon et al., 2019). An airborne vehicle, by contrast, could fly at low altitudes to improve the acquisition of CH_4 concentration (Elder et al., 2020; Wolff et al., 2021a) and estimate CH_4 emission from strong sources by the cross-sectional flux method or the Gaussian dispersion method. However, it has strict requirements for the flight track (downwind direction) and amount of measured CH_4 concentration data. Most ground-based sensors have the advantage of sampling the concentration around the source continuously, but they could only collect data near the surface or measure column concentration (Zhou et al., 2021; Robertson et al., 2017; Caulton et al., 2017), which are insufficient to generate the distribution characteristic of the emission source. Ground-based differential absorption LIDAR could obtain the CH_4 profile concentration in different altitudes, whose data is suitable as the input of the emission-retrieval model (Shi et al., 2020a), but it has high requirements in terms of hardware performance and system stability (Shi et al., 2020b). An unmanned aerial vehicle (UAV) could reach any location rapidly around the CH_4 sources, which could sample CH_4 concentration with location information (Nathan et al., 2015b; Iwaszenko et al., 2021), when equipped with an in-situ gas sensor. It could also acquire the distribution characteristics with adequate data, which is beneficial to retrieving the emission rate.

In 2017, we developed an UAV-based active AirCore system, which could sample atmospheric CO2, CH_4, and CO with high accuracy (Andersen et al., 2018), aiming to retrieve greenhouse gases emission for strong sources. The most urgent issue we need to address is developing an emission quantification model with high applicability. This model should have less uncertainty in retrieved result and be comply with the actual emission dispersion characteristics of the studied emission sources. Mass-balance method has been applied in determining CH_4 emissions based on UAV-based samples (Allen et al., 2018). Emission rates calculated by this method contain large uncertainty because the main kernel is Kriging interpolation (Nathan et al., 2015a), which can cause obvious uncertainty in representing the actual feature of diffusion. The Gaussian dispersion model has also been applied in retrieving gas emission from strong sources (Shah et al., 2019; Ma and Zhang, 2016), and it is also used to model CH_4 diffusion in this study. However, existing emission-retrieval methods based on Gaussian dispersion model need priori information on key diffusion parameters (Nassar et al., 2021), which cancan not be regarded as certain values in different circumstances. Moreover, the measurements accuracy of auxiliary meteorological data also has a great impact on CH_4 emission calculation.

To end this, we developed herein a model to overcome these shortcomings, named GA-IPPF. combines the advantages of genetic algorithms (GA) and interior point penalty functions (IPPF). GA would modeled the fitness function as a process of biological evolution(Yuan and Qian, 2010), which would be

https://doi.org/10.5194/acp-2022-180
Preprint. Discussion started: 7 June 2022

Atmospheric Chemistry and Physics Discussions

used to calculate the potential solutions in Gaussian dispersion model. IPPF would find the minimum of the criteria in setting domain (Kuhlmann and Buskens, 2018), which can help us achieve global optimal solutions for concerned parameters. Finally, GA-IPPF could calculate the diffusion parameters without prior information and reduce the impact of meteorological data on the calculated CH_4-emission rate.

We introduced the structure of our developed GA-IPPF in detail in section 2. In section 3, we evaluated the performance of GA-IPPF in field campaign around a coal mine ventilation shaft by using AirCore system in seven Flights. Then, we discussed the comparisons between different quantification methods for CH_4 emission, and evaluated the potentials of GA-IPPF when the fifth generation of ECMWF atmospheric reanalysis of the global climate (ERA5) database only available. In section 4, we validate the accuracy of GA-IPPF in Observing System Simulation Experiments (OSSE), and evaluated the uncertainty in retrieved emission rate of CH_4.

2.Data and methods

2.1. Active AirCore System

The active AirCore system comprises a ~50 m coiled stainless-steel tube that works in conjunction with a micropump and a small pinhole orifice (45 μm) to sample air along the trajectory of a drone. If the pressure downstream of the orifice is more than half of that of the upstream (ambient) pressure, a critical flow through the orifice is obtained. This means that the flow rate depends only on two variables, namely, the air temperature and the upstream (ambient) pressure, both of which are monitored during the flight. After obtaining the air sample, the sample is analyzed on a cavity ring down Spectrometer model G2401-m for CO_2, CH_4, and CO. For CH_4, the accuracy of samples is ±0.02 parts per million (ppm). The active AirCore system is controlled using an Arduino-built data logger, which records the temperature inside the carbon fiber housing. It also records the ambient temperature, ambient pressure, relative humidity, and pressure downstream of the pinhole orifice to ensure that critical flow is achieved. The datalogger also logs the GPS coordinates. The weight of the active AirCore system is ~1 kg. The active AirCore system is attached to a DJI Inspire Pro 1, which is capable of providing flights of ~12 min.

2.2. Meteorological measurements

A radiosonde (Sparv Embedded AB, Sweden, model S1H2-R) measures ambient temperature, ambient pressure, ambient relative humidity, wind speed, and wind direction. The detection range of the temperature sensor is –40 °C to +80 °C, with an accuracy of 0.3 °C. The pressure sensor has a detection range of 300–1100 mbar, with an accuracy of 1 mbar. The relative humidity sensor measures in the range of 0%–100%, with an accuracy of approximately 2%. Owing to the good connection between the radiosonde and satellites, we assume that the uncertainty in the wind direction is low. The wind speed can be estimated within a range of 0–150 m/s, with an uncertainty of approximately 5%. If the wind-speed reading is less than 4 m/s, a minimum uncertainty of 0.2 m/s is given. The radiosonde is lifted by a ~30 L helium-filled balloon and is tethered onto a fishing line for easier retrieval after making a vertical profile.

2.3 Emission retrieve model

2.3.1. Gaussian dispersion model

The Gaussian dispersion model is used to analyze the CH_4 fugitive from the coal mine in this work. The location of emission source is regarded as the coordinate origin; X-axis is the direction of the downwind, Y-axis is cross-wind direction, and Z-axis is the altitude above the ground. Based on the established coordinate system, the Gaussian plume could be modeled by Equation 1:

$$C(x,y,z)=\frac{q}{2\pi u\sigma_y\sigma_z}\exp(\frac{-(y)^2}{2\sigma_y^2})\left\{\exp(\frac{-(z-H)^2}{2\sigma_z^2})+\alpha\cdot\exp(\frac{-(z+H)^2}{2\sigma_z^2})\right\}+B \qquad (1)$$

https://doi.org/10.5194/acp-2022-180
Preprint. Discussion started: 7 June 2022

Atmospheric Chemistry and Physics Discussions

$$\sigma_y = a \cdot x^b \tag{2}$$

$$\sigma_z = c \cdot x^d \tag{3}$$

Where C is the concentration of CH_4 (g/m^3), q (g/s) is the emission rate of coal mine, u is the mean wind speed around the stack (m/s), H is the effective stack height, σ_y is the dispersion coefficient in the horizontal direction, σ_z is the dispersion`n coefficient in the vertical direction, u is the wind speed (m/s), and B is the background concentration of CH_4. Moreover, α is the reflection index of the measurement phenomenon; and x, y, and z are the positions of the samples in the determined coordinate system.

2.3.2.GA-IPPF model.

First, the genetic algorithm (GA) kernel calculates Q and other dispersion parameters with a first guess (Liu and Michalski, 2016). It guarantees that the unknown parameters would be retrieved through the global optimum solution, as shown in Fig.1. Then, the results calculated by GA serve as initial input parameters and constraints in the IPPF model, and actual values of the concerned parameters are retrieved by IPPF, detailed information could be found in S1 (supplement).

Based on the Gaussian dispersion model, auxiliary meteorological data, location information, and CH_4 samples, we determine the unknown parameters in equations 1 to 3 by using GA, including q, H, a, b, c, d, and α, lower boundary and upper boundary would constraint these parameters in logical range. First, the locations and concentration of CH_4 samples and wind serve as an initial input of equation 1. Then, the fitness value evaluates the applicability of the calculated parameters in each step. We define the fitness value as

$$F = \sum_{i=1}^{n} (C_m^i - C_s^i)^2 \tag{4}$$

$$C_s^i(x,y,z) = \sum_{i=1}^{n} \frac{q'}{2\pi u' \sigma_y' \sigma_z'} \exp\left(\frac{-(y)^2}{(\sigma_y')^2}\right)\left\{\exp\left(\frac{-(z-H')^2}{(\sigma_z')^2}\right) + \alpha' \cdot \exp\left(\frac{-(z+H')^2}{(\sigma_z')^2}\right)\right\} + B' \tag{5}$$

Where F is the fitness value; C_m^i is the sample CH_4 concentration; i is the number of samples; C_s^i is the simulated concentration of CH_4 in the location of samples calculated by equation 5; and q′, u′, σ_y', σ_z', H′, α′, and B′ are the calculated CH_4-emission rate, wind speed, diffusion parameters, emission height, reflect index, and background CH_4 concentration, respectively, acquired from the "Mutation" in Fig.1. When f is less than the threshold value (1×10^{-5}) of the fitness value, the corresponding parameters are treated as the results of output.

IPPF rebuilds the inequality constraint conditions to the unconstrained solution process. It forces the start point to satisfy the constraints, as shown in equation 6.

$$minF\left(x, r_k\right) = f(x) + r_k B(x) \tag{6}$$

Where f(x) is the unconstrained equation, and r_k is the coefficient of the constrained equation B(x). When the solution parameters are out of the constraints, r_kB(x) is large, thereby ensuring that the final solution is feasible under the inequality constraint conditions.

To obtain the inequality constraints, GA is repeated 1000000 times, and the mean values of the calculated wind speed, wind direction, H, a, b, c, d, and α are treated as the initial input of IPPF model. The domains of H, a, b, c, d, and α are determined by two times the standard deviation of the corresponding results in GA. The constraint values of wind speed and direction are set according to the

https://doi.org/10.5194/acp-2022-180
Preprint. Discussion started: 7 June 2022

Atmospheric Chemistry and Physics
Discussions

precision of actual measurements, m±σ，whereas m is the measured value of wind speed or wind direction, and σ is their precision. Actual B values are considered to be within 1800–2500 ppb. Then, the Pearson correlation coefficient (R) values of the actual samples and simulated values work as the criterion in the solution process of equation 7.

$$R=\frac{\sum_{i=1}^{n}\left(C_s^i-\overline{C_s}\right)\left(C_m^i-\overline{C_m}\right)}{\sqrt{\sum_{i=1}^{n}\left(C_s^i-\overline{C_s}\right)^2}\sqrt{\sum_{i=1}^{n}\left(C_m^i-\overline{C_m}\right)^2}} \tag{7}$$

The results are treated as the final retrieved values of the concerned parameters when the R reaches the maximum.

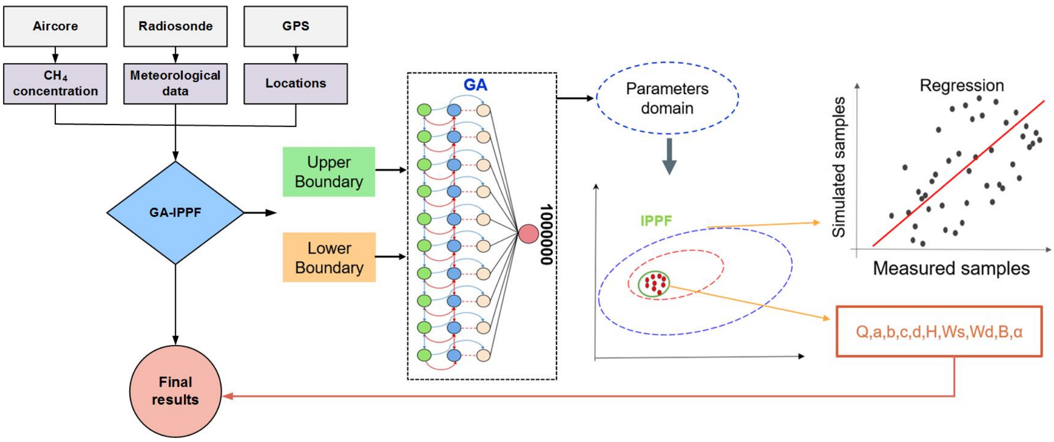

Fig.1. Flow chart of GA-IPPF model.

2.4. Measurement Site

The Pniówek coal mine (49.975° N, 18.735° E) is a large mine in Pniówek, Silesian Voivodeship, Poland, which is 190 km southwest of the capital Warsaw, see Fig.2. It has a large coal reserve estimated to be about 101.3 million tons. Its coal production is about 5.16 million tons per year.

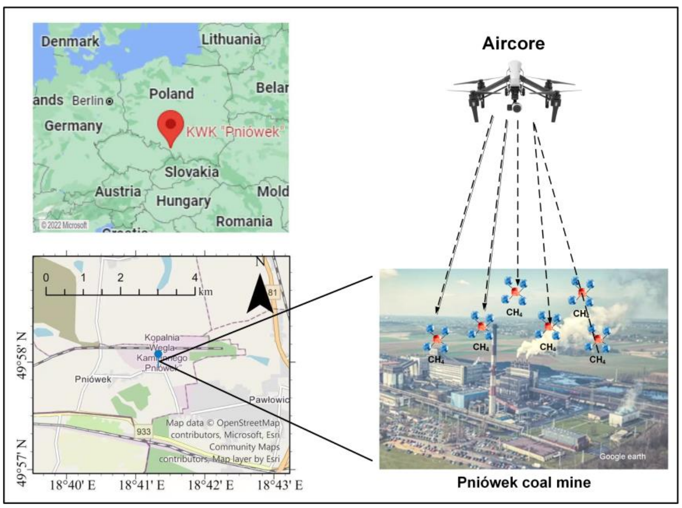

Fig.2. The Pniówek coal mine in Poland

https://doi.org/10.5194/acp-2022-180
Preprint. Discussion started: 7 June 2022

Atmospheric Chemistry and Physics Discussions

3. Results

3.1. Actual experiments

Fifteen active AirCore flights around Pniówek coal mine are collected successfully on August 18, 2017 and August 21, 2017. The sample data in Flight 6 (18/8/2017) and Flight 15 (21/8/2017) are used to evaluate the GA-IPPF model, as shown in Fig. 3.

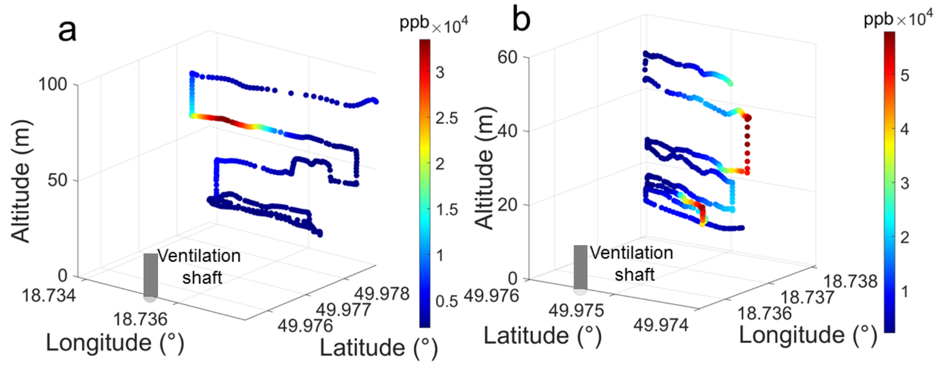

Fig. 3. Samples of CH_4 in two Flights: (a) Flight 6 and (b)Flight 15.

In Flight 6, the AirCore system collects CH_4 around the coal spirally from 0 m to 98 m, for a total of 376 samples, and the measurement period is 7 min, ranging from 1980.1 ppb to 49 113.9 ppb. In Flight 15, the AirCore system collected a total of 400 samples, and the measurement period is 9 min, ranging from 2131.7 ppb to 57 265.3 ppb. Both Flights show high spatial variability in CH_4 exhaust from coal mine. Subsequently, we input the wind speed, wind direction, location information, and CH_4 samples collected from Flights into the GA-IPPF model. To express the final retrieved emission (Q) in g/s, the dry-air mixing ratio of CH_4 (ppb) is transformed into mass concentration m (mg/m^3) as follows:

$$m = C \cdot \frac{M_{CH4}}{M_{Air}} \cdot 10^{-3} \tag{8}$$

Where M_{CH4} is the molar mass of CH_4, and M_{air} is the molar mass of air.

The retrieved results are shown in Table 1, the uncertainty is presented in Discussion in detail. Notably, the emission height in Flight 15 is larger than that of Flight 6, which may be caused by the difference in thermal energy and vertical wind speed of the two flights. The background concentrations of CH_4 are 1.55 and 1.57 mg/m^3 in Flights 6 and 15, respectively, which show little difference. The dates of the two Flights are very close, so the background concentration of CH_4 in two days have nearly the same seasonal characteristics. The exhaust gases of coal mine are emitted through the stack with effective emission heights of 59.3 and 36.4 m, respectively.

To evaluate the rationality of the retrieved results, these parameters are used to simulate CH_4 diffusion from the Pniówek coal mine according to equation 1. The comparison between simulated CH_4 concentration and actual samples in the same locations is shown in Fig.4.

Table 1. Results calculated by GA-IPPF model

Parameters	Flight 6	Flight 15
Initial wind speed (m/s)	4.5	4.1
Initial wind direction (°)	310	125.4
Emission intensity (kg/hour)	693.3±34.2	958.9±57.4
Wind speed (m/s)	3.25	3.20

https://doi.org/10.5194/acp-2022-180
Preprint. Discussion started: 7 June 2022

Atmospheric Chemistry and Physics Discussions

Wind direction (°)	349.6°	128.1
a	0.22	0.31
b	0.90	0.90
c	0.006	1.50
d	1.29	0.38
B (mg/m^3)	1.55	1.56
Emission height (m)	59.3	36.3
Reflection index	0.85	1.0

Then, we also calculated the difference between the actual measured points and simulated ones as

$$D_c = C_s - C_m \tag{9}$$

Where D_c is the difference of CH_4 concentration between actual measured and simulated ones. C_s is simulated CH_4 concentration (mg/m^3), and C_m is simulated CH_4 concentration (mg/m^3).

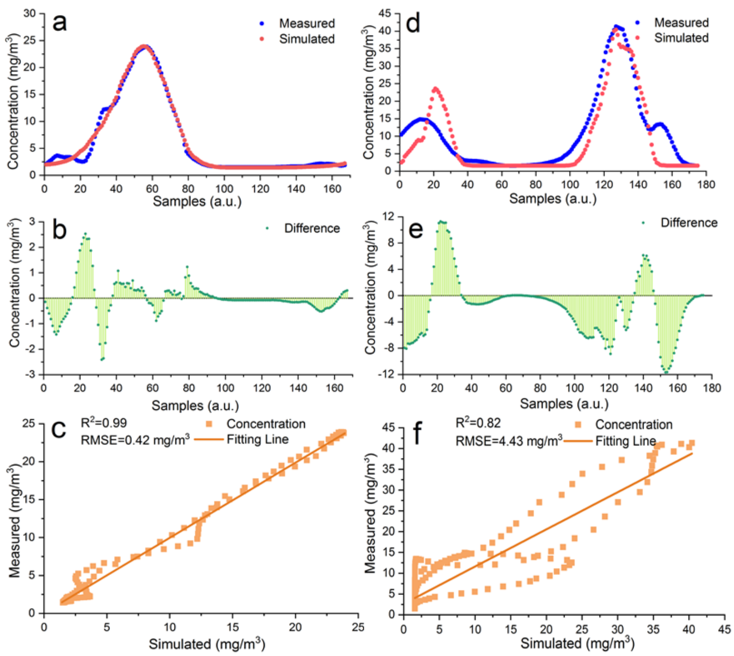

Fig. 4. Comparison between the measured samples and the simulated ones based on the parameters in Table 1: (a). Flight 6 and (d) Flight 15. The difference of simulated CH_4 concentration and actual measured ones: (b) Flight 6 and (e) Flight 15. Correlation Analysis: (c) Flight 6 and (f)Flight 15.

As shown in Fig. 4(a), the tendency of the simulated concentration data is consistent with the measured ones in Flight 6. The largest value (NO.55) of the measured CH_4 concentration is 23.9 mg/m^3, whereas the simulated one is 23.8 mg/m^3 on same location, with only 0.42% bias. Dc is ranging from -2.4 to 2.3 mg/m^3 in Flight 6 (see Fig.4(b)), this little bias indicates that the simulated result is reasonable. The R2 of the measured samples and simulated ones is 0.99, and the root mean square error (RMSE) is 0.42 mg/m^3. These indicate that the GA-IPPF model could correctly rebuild the diffusion of CH_4 in Flight 6. Fig.4(d) shows a slight difference between the two items in the first and third peaks. The GA-IPPF method could adjust more weights to the samples with higher concentration (NO.100 to 150 in Flight 15) to get the global optimal solution of the relevant parameters, leading to the low fitness of the first peak

https://doi.org/10.5194/acp-2022-180
Preprint. Discussion started: 7 June 2022

in Fig. 4(e). In general, the tendency of the simulated values remains consistent with that of the actual samples in Flight 15, especially for the points in the second peak. R2 and RMSE of the measured samples and simulated ones in Flight 15 also show the excellent diffusion reconstruction by GA-IPPF.

3.2 Comparison with other methods

To investigate the difference between our proposed emission model and the others, three methods have been applied to estimate CH_4 emission in all Flights, including mass-balance approach, nonlinear least square fit (NLSF), and facility emission.

Mass-balance approach quantifies CH_4 emission by calculating the cross-sectional flux perpendicular to the wind direction (Krings et al., 2018). First, a two-dimensional plane is selected according to the amount of CH_4 samples. Second, the two-dimensional plane is divided into a grid of equal spatial resolution. Third, CH_4 samples are regarded as origin points to interpolate full grids defined by the Kriging interpolation scheme (Mays et al., 2009). Finally, the emission rate of the CH_4 source is calculated by

$$F_{(CH4)} = \iint v \sin(\alpha) \cdot (C_{(x,z)} - C_{bg}) dxdz \tag{10}$$

Where v is the wind speed, α is the angle between wind direction and the two-dimensional plane, $C_{(x,z)}$ is the density of CH_4 in each grid, and C_{bg} is the background of CH_4 in each grid. The uncertainty analyses of this method are detailed in Nathan et al. (Nathan et al., 2015a).

NLSF and the combination of NLSF with Gaussian diffusion model are also extensively used for point-source emission retrieval (Zheng et al., 2020; Wolff et al., 2021b). In this study, NLSF is used to estimate Q in each Flight by fitting the unknown parameters in equation 1.

Andersen et al. also developed an inverse Gaussian approach to quantify CH_4 emissions from coal mine based on the same Flights (Andersen et al., 2021). Firstly, the Gaussian dispersion is built as

$$C(x,y,z) = \frac{q}{2\pi u \sigma_y \sigma_z \cos(\theta)} \exp\left(\frac{-(y)^2}{2\sigma_y^2}\right) \left\{ \exp\left(\frac{-(z-H)^2}{2\sigma_z^2}\right) + \exp\left(\frac{-(z+H)^2}{2\sigma_z^2}\right) \right\} \tag{11}$$

Where θ is the angle between the wind direction and the perpendicular line of the flight trajectory. This model does not include the item of background of CH_4. Furthermore, σ_y and σ_z are treated as certain values in equation 11.

Facility-emission data and hourly CH_4 emission from shaft are calculated by measuring raw CH_4 concentration and air flux through the shafts, following the equation below

$$Q_{Inventory} = \frac{P \cdot V_{flow}}{R \cdot T} \rho \tag{12}$$

Where V_{flow} is the volumetric flow rate of CH_4 in $m^3 s^{-1}$, given by the air flow rate (scaled by a constant factor of 0.95 to account for the ~5% additional air flow not coming from the ventilation shaft) multiplied by the CH_4 concentration, and P, R, T, ρ are the atmospheric pressure in Pa, the universal gas constant in $J\ mol^{-1}\ K^{-1}$, the ambient temperature in K, and the molar density of CH4 in $g\ mol^{-1}$ (16.043 $g\ mol^{-1}$), respectively.

CH_4 emission rates estimated using hourly facility-emission data for 18 August 2017 and 21 August 2017 are 1655.3 ±479.45 and 913.2 ±285.4 kg/hour, respectively, as shown in Fig. 5.

https://doi.org/10.5194/acp-2022-180
Preprint. Discussion started: 7 June 2022

Atmospheric Chemistry and Physics
Discussions

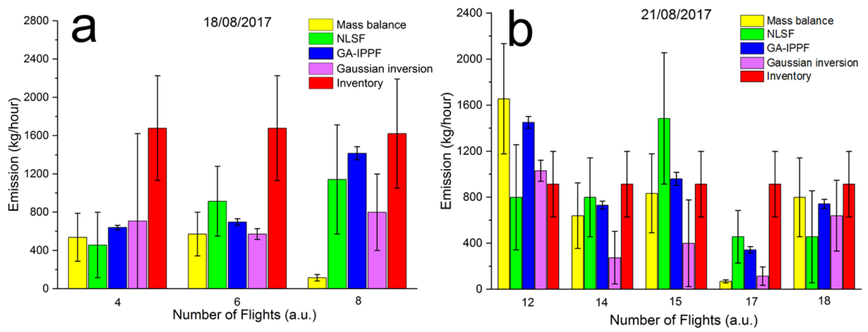

Fig. 5. Quantified CH_4 emission by different methods based on the collected data: (a) August 18, 2017 and (b) August 21, 2017. The results of CH_4 emission rate calculated by Mass balance and Inverse Gaussian refer to Andersen et al.

As shown in Fig. 5, Flights 4, 6, and 8 are measured on 18 August 2017, whereas Flights 12, 14, 15, 17, and 18 are measured on 21 August 2017. Fig.5(a) shows that the CH_4-emission rates calculated by mass balance are smaller than the inventory estimation in all Flights. In Flight 8, q retrieved by mass balance is extremely lower than those quantified by other methods, whereas q retrieved by GA-IPPF model (1415.5±68.5 kg/hour) shows only a slight difference from the inventory. As shown in Fig.5(b), CH_4 emissions retrieved by mass balance, inverse Gaussian, and GA-IPPF model are overestimated compared with the inventory in Flight 12. Mass balance and inverse Gaussian method also show obviously underestimated q in Flight 17. Estimations of retrieved CH_4 emission in Flight 18 show consistency among methods of mass balance, GA-IPPF, and inverse Gaussian. The CH_4-emission rate of coal generally has significant variability in each measurement, even on the same day. Mass balance is very sensitive to the size settings of grids, and different height and length settings can affect the concentration distribution across the cross-section. NLSF has a high-accuracy requirement for wind measurements, and errors on these measurements have a linear influence on the final emission estimation. Notably, the standard errors of q quantified by GA-IPPF are always the least among these methods, indicating the stability of the model we developed.

3.3 Application of Reanalysis meteorological database in GA-IPPF model

Wind speed and wind direction acquired by the radiosonde or weather station are two main parameters in GA-IPPF. However, additional sensors are bound to increase the cost and difficulty during actual CH_4-emission measurements. To explore the possibility of weather reanalysis data instead of actual wind measurement by sensors, we use 10 m U and V wind components from the ERA5 meteorological reanalysis database (spatial resolution is 0.1°×0.1°, and temporal resolution is 1 h) developed by the European Centre for Medium-range Weather Forecast (Hersbach et al., 2020) to evaluate GA-IPPF model. However, the wind directions from ERA obviously differ from the actual measurements during the Flights. Hence, we determine the wind direction by using the CH_4 samples, for example, the line between the shaft and the location of the maximum value of samples in the same heights is treated as the downwind direction, whose uncertainty is set as 50°. Wind speed from ERA is used for the CH_4-emission calculation, and the uncertainty is supposed as 2 m/s. Even initial wind speed and direction obviously differ between the two sources; however, the GA-IPPF model adjusts them into reasonable ranges. The results of q during all Flights retrieved by two meteorological data sources have been evaluated, as shown in Table 2.

https://doi.org/10.5194/acp-2022-180
Preprint. Discussion started: 7 June 2022

Table 2. Retrieved CH_4 emission by ERA meteorological data

Flights	Actual (kg/hour)	ERA5(kg/hour)
4	639.3±22.8	684.9±34.2
6	693.3±34.2	730.6±57.7
8	1415.5±68.5	1643.8±102.7
12	1499.8±57.1	1506.8±79.9
14	730.6±34.2	570.8±45.7
15	958.9±57.4	590.4±68.5
17	342.5±34.8	388.1±57.1
18	742.0±0.4	799.1±57.4

Table 2 shows that the values of quantified q between the two meteorological sources are within 20% in the same Flight. The standard errors of q retrieved by the ERA5 database are larger than those from actual measurements, which depends on the accuracy of the reanalysis of wind speed and wind direction. Thus, it has no requirement of additional equipment except for the AirCore system

We also explored the reason behind the little difference of the calculated emission rate by the two sources of meteorological data. The concerned parameters in Flight 6 and Flight 15 calculated based on ERA5 meteorological data were presented in Table 3.

Table 3. Results calculated ERA5 meteorological data

Parameters	Flight 6	Flight 15
Initial wind speed (m/s)	2.6	4.1
Initial wind direction (°)	300	120
Emission intensity (kt/hour)	730.6±57.1	590.4±68.5
Wind speed (m/s)	2.99	4.52
Wind direction (°)	349.4°	128.1
a	0.28	0.18
b	0.90	0.93
c	0.01	0.13
d	1.26	0.84
B (mg/m^3)	1.56	1.57
Emission height (m)	60.2	36.0
Reflection index	0.80	0.71

The initial wind speed and wind direction in Table 3 are obviously different from those in Table 1. However, the calculated wind directions are nearly the same based on the two sources of meteorological data. Diffusion parameters and emission height also show less difference in two Tables (Table 1 and Table 3). It is worth noting that the wind speed and reflection index would be adjusted to reach the global solution by GA-IPPF model, which leads to little bias for the emission rate of CH_4 in Table 2.

https://doi.org/10.5194/acp-2022-180
Preprint. Discussion started: 7 June 2022

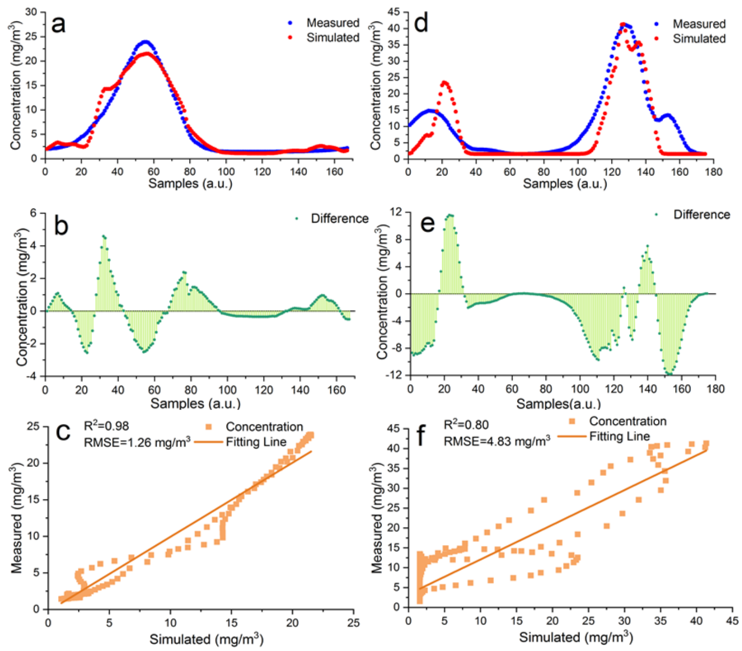

Fig. 6. Comparison between the measured samples and the simulated ones based on the ERA5 meteorological data: (a). Flight 6 and (d) Flight 15. The difference of simulated CH_4 concentration and actual measured ones:(b) Flight 6 and (e)Flight 15. Correlation Analysis: (c) Flight 6 and (f)Flight 15.

The simulated concentration of CH_4 in Flight 6 and Flight 15 calculated by parameters in Table 3 are shown in Fig.6. In Fig.6(a). The consistency between the actual samples and the simulated ones is slightly lower than that in Fig.6(a), D_c ranges from -2.4 to 4.3 mg/m^3, which is an acceptable bias as only 6 points exceed 2.3 mg/m^3. The R^2 (0.98) of measured samples and simulated ones is almost the same as that in Fig.4(c), while RMSE is nearly three times than that in Fig.6(c). In Fig.6(d), the tendency of simulated CH_4 concentration is similar to Fig.4(d). D_c ranges from -11.9 to 11.6 mg/m^3, which is nearly the same as the result in Fig.4 (e). It's worth nothing that D_c simulated by ERA meteorological data is slightly larger on samples (NO.1 to 20) compared with that in Fig.4 (e). The R^2 and RMSE in Fig. 6(f) indicate that the retrieved results using ERA data are less accurate than those using actual measured meteorological data. In summary, though we set large uncertainties in ERA5 meteorological data, GA-IPPF can still guarantee reasonable and adequate accuracy for the retrieved emission rate and diffusion parameters.

4.Discussion

4.1. Validation of performance of GA-IPPF model through OSSEs

Firstly, the dispersion of CH_4 emission from a coal is simulated by equation 1, and the dispersion parameters are shown in Table 4. To make the simulations close to the actual measurement scenarios, random errors were added to the CH_4 concentration samples (5%), wind speed (± 0.3 m/s), and wind direction (± 20°). The spatial resolution of the supposed samples is 10 m, and 70 samples were selected from the simulated dispersion to represent the data acquired by the UAV-based AirCore. Then, the concerned parameters are retrieved by the GA-IPPF method. The input parameters include hypothetical wind speed, wind direction, and 70 samples, as shown in Fig. 7. Simulations were repeated 10 000 times,

https://doi.org/10.5194/acp-2022-180
Preprint. Discussion started: 7 June 2022

Atmospheric Chemistry and Physics
Discussions
Open Access

and the average values of the corresponding parameters are treated as the "Retrieved" results in Table 4.

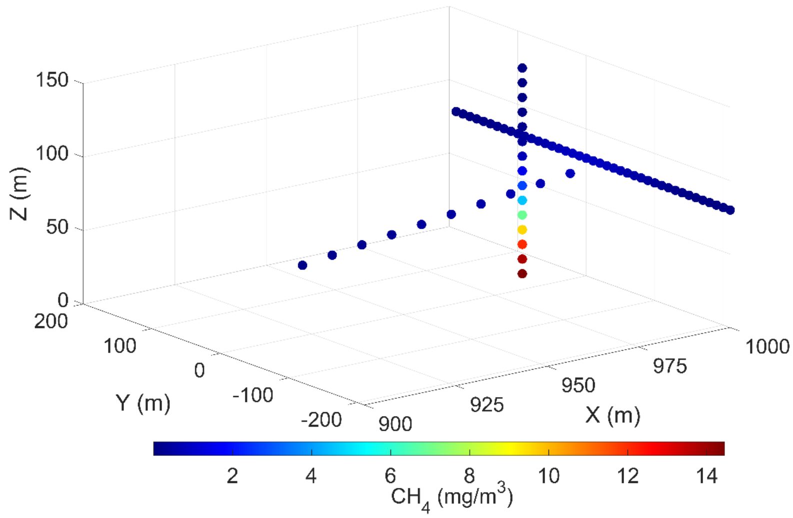

Fig. 7. The determined 70 CH_4 samples in simulations

Table 4. The parameters setting in dispersion simulation and the retrieved results by GA-IPPF

Parameters	Lower boundary	Upper boundary	Actual	Retrieved
Emission intensity (g/s)	0	100000	300	300.5±0.01
Wind speed (m/s)	0	100000	3	3±0.01
Wind direction (°)	70	110	90	90±0.01
a	0	1000	0.11	0.13±0.02
B	0	1000	0.9	0.9±0.02
c	0	1000	0.1	0.12±0.01
d	0	1000	0.82	0.8±0.01
B (ppb)	1700	2500	1900	1900±3
Emission height (m)	0	150	20	19.7±1.2
α	0	1	0.9	0.89±0.03

"Actual" means the set values of parameters, and "Retrieved" means the average values of parameters retrieved by GA-IPPF model through 10 000 times of simulation.

As shown in Table 1, q retrieved by GA-IPPF has only 0.17% bias compared with the set values. Emission height only has 0.3 m bias in terms of the set one, and the uncertainty is only 0.6% to 20 m. Other retrieved parameters also show high consistency with the original settings.

4.2. Stability analyses

The necessary input parameters in GA-IPPF contain meteorological data (wind speed and direction), accuracy of CH_4 samples, and amount of CH_4 samples. In equation 1, wind speed has a nearly linear relationship with the emission estimation. Wind speed is also an important factor that determines atmospheric stability according to the Pasquill–Gifford method (Venkatram, 1996) as it affects the diffusion parameters of σ_y and σ_z. The coordinate is built according to the wind direction, which is defined as the plane coordinates of CH_4 samples. According to equations 2 to 3, errors in wind-direction measurement led to wrong σ_y and σ_z on each position of samples. CH_4 samples are the most important

https://doi.org/10.5194/acp-2022-180
Preprint. Discussion started: 7 June 2022

Atmospheric Chemistry and Physics
Discussions

factors to determine the Gaussian diffusion. The accuracy of samples influences the judgment of "fitness" in the GA process. More samples collected in different positions help rebuild the spatial-distribution characteristics of the plume because it provides larger possibility for fitting process in IPPF and helps determine the optimum solution. To evaluate the influence of errors in the measurements of necessary parameters on the final retrieved results, the same settings in Table 1 are used as actual results. The performance of the GA-IPPF model with additional random errors in each parameter was simulated 10 000 times, as shown in Fig. 8.

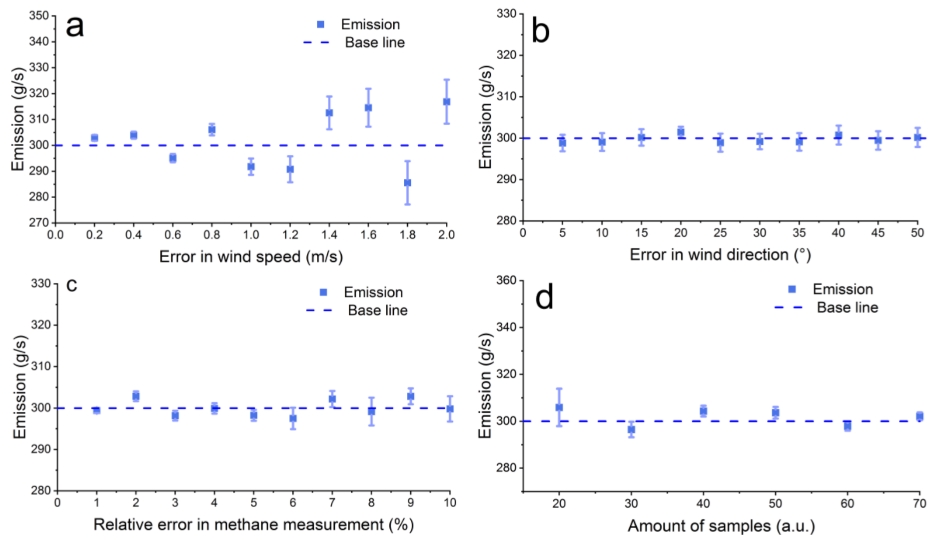

Fig. 8. Influence of accuracy of parameters on retrieved emission results. The baseline represents the emission rate setting of CH_4, 300 g/s: (a) wind speed, with additional error ranging within 0.2–2 m/s and an interval of 0.1 m/s, (b) wind direction, with additional error ranging within 5°–40° and an interval of 5 °, (c) accuracy of CH_4 samples, with additional error ranging within 0.5%–5.0% and an interval of 0.5%, and (d) amount of CH_4 samples, randomly selected as 20–70 among the defined 70 samples.

In Fig.8(a), the mean value of q retrieved by GA-IPPF is nearly the same as the baseline if the error in wind speed is less than 0.4 m/s and the maximum bias to the baseline is 16.3 g/s. Fluctuation of q occurs obviously if the error in wind speed exceeds 0.4 m/s. The standard errors of q are positively correlated with the values of errors in wind speed, indicating that the accuracy of wind-speed measurements largely influence the stability of the GA-IPPF model. This model has a self-adjustment function for wind speed; for example, when the initial wind speed is 3 m/s, the maximum standard error of q is only 8.5 g/s (3.5% to the 300 g/s) when the additional error of wind is 2 m/s (66.7% to 3 m/s).

The retrieved q shows less sensitivity to errors in wind direction (see Fig.8(b)). When errors in the wind direction are 5° to 40°, all biases of q are within 1.1 g/s and the standard errors are around 2.3 g/s. Wind direction determines the spatial location of the sampling point, and wrong location information leads to distinct errors in emission estimation. GA-IPPF shows highly accurate ability in the wind direction to obtain the global optimum solution.

Sampling accuracy has small impact on the retrieved q within different settings in CH_4 samples' accuracy, see Fig.8(c). Standard deviation is positively correlated with errors in CH_4 measurements. The standard deviation is 3.1 g/s when the measurement error reaches 5%. Notably, the uncertainty of CH_4

https://doi.org/10.5194/acp-2022-180
Preprint. Discussion started: 7 June 2022

samples measured by UAV-based AirCore system is far less than 5%. The AirCore system could acquire more than 70 CH_4 samples in actual feasible measurements, thereby guaranteeing the accuracy of the retrieved CH_4 emission by coal to exceed 99.2%.

The number of measurement points obviously influences the final accuracy of q by the GA-IPPF model (see Fig.8(d)). It has a bias of 5.9 g/s to 300 g/s when n is 20. The accuracy of q and the standard error are negatively correlated with n, which provides the number of criterion for the fitting process in the retrieval model. Hence, n directly influences the retrieved results. The AirCore system has the advantage of continuous sampling during flight, which integrates the atmospheric signals along the flight path and helps reduce the uncertainty in the retrieved q. Besides, the smoothing of the atmospheric signal also reduces the spatial resolution of the measurements, which needs to be considered during the optimization.

IPPF can suitably solve the problem of inequality constraints, and the calculated solution guarantees the calculated parameters to be within the feasible region. In this section, the performance of the GA-IPPF model and the influence of the four key input parameters were discussed.

Uncertainty Analyses

The uncertainties in CH_4-emission estimations derived from the measurements of meteorological data and CH_4 samples in the discussed Flights. As shown in Fig. 8, n is the largest source that contributes to the uncertainty in emission calculation. The accuracy of AirCore samples, wind speed, and wind direction should also be of concern. Therefore, the total uncertainty in actual CH_4 emission retrieved could be calculated as

$$\varepsilon_t = \sqrt{\varepsilon_n^2 + \varepsilon_m^2 + \varepsilon_w^2 + \varepsilon_d^2} \quad (13)$$

Where ε_t is the total uncertainty of Q estimation. In this section, ε_n, ε_m, ε_w, and ε_d are the uncertainty caused by n, accuracy of CH_4 samples, wind speed, and wind direction, respectively. Results in Fig.8 are used to determine the values of ε_n, ε_m, ε_w, and ε_d in each Flight.

5.Conclusion

CH_4 emissions from coal are inconsistent even with short time differences. They usually show large differences for different mining volumes and types. Enhancement in CH_4 by the emission source is much larger than the background concentration, and the distribution of leak gas shows an obvious spatial difference. Hence, the retrieval time needs to be shortened for each emission measurement. AirCore has high portability and flexibility in measuring CH_4 concentration around emission sources, accompanied by the GA-IPPF model, which is excellent to calculate CH_4 emission from coals or other point sources. This program can help improve the accuracy of CH_4 emission estimations from coals, especially for developed countries that even lack inventories of gas emission. It can also help governments evaluate the fugitive CH_4-emission rate during mining and equationte policies to promote the innovation of mining equipment and technology. We demonstrated that the UAV-based AirCore system can help us to rebuild the diffusion of CH_4 with flexibility and high sampling rate. The GA-IPPF model could restrict the calculated emission details within a reasonable range. The recommended model is appropriate for quantifying local sources based on the advanced hardwares, such as Aircore system, Lidar as well as vehicle-based in-situ measurement. What's more, this model also has great potential in the point-source quantitation of other gases, such CO_2 and SO_2.

Author contributions. HC, XM, TS planned the campaign; TS, TA, HC, HM performed the measurements; TS and ZH analyzed the data; GH and TS wrote the manuscript draft; CC, HZ, and WG reviewed and edited the manuscript.

Competing interests. The authors declare that they have no conflict of interest.

Acknowledgements. This work was supported by the National Natural Science Foundation of China (Grant No.41971283, 41801261, 41827801, 41901274, 41801282, 42171464), the National Key Research and Development Program of China (2017YFC0212600), The Key Research and Development Project of Hubei Province (2021BCA216), the Open Research Fund of National Earth Observation Data Center(NODAOP2021005).

References

Allen, G., Hollingsworth, P., Kabbabe, K., Pitt, J. R., Mead, M. I., Illingworth, S., Roberts, G., Bourn, M., Shallcross, D. E., and Percival, C. J.: The development and trial of an unmanned aerial system for the measurement of methane flux from landfill and greenhouse gas emission hotspots, Waste.Manage., 87, 883–892, https://doi.org/10.1016/j.wasman.2017.12.024, 2019.

Andersen, T., Scheeren, B., Peters, W., and Chen, H. L.: A UAV-based active AirCore system for measurements of greenhouse gases, Atmos.Meas.Tech., 11, 2683–2699, https://doi.org/10.5194/amt-11-2683-2018, 2018.

Andersen, T., Vinkovic, K., de Vries, M., Kers, B., Necki, J., Swolkien, J., Roiger, A., Peters, W., and Chen, H.: Quantifying methane emissions from coal mining ventilation shafts using an unmanned aerial vehicle (UAV)-based active AirCore system, Atmos.Environ.,12,100135, https://doi.org/10.1016/j.aeaoa.2021.100135, 2021.

Cardoso-Saldaña, F. J. and Allen, D. T.: Projecting the temporal evolution of methane emission s from oil and gas production sites, Environ.Sci.Technol., 54, 14172–14181, https://doi.org/10.1021/acs.est.0c03049, 2020.

Caulton, D. R., Qi, L., Bou-Zeid, E., Lu, J., Zondlo, M. A. J. A. C., and Physics: Improving Mobile Platform Gaussian-Derived Emission Estimates Using Hierarchical Sampling and Large Eddy Simulation, Atmos. Chem. Phys. Discuss.,18, 15 145–68, https://doi.org/10.5194/acp-2017-961, 2017.

Elder, C. D., Thompson, D. R., Thorpe, A. K., Hanke, P., Walter Anthony, K. M., and Miller, C. E.: Airborne Mapping Reveals Emergent Power Law of Arctic Methane Emissions, Geophys. Res. Lett., 47, e2019GL085 707, https://doi.org/10.1029/2019GL085707, 2020.

Feng, L., Palmer, P. I., B?Sch, H., Parker, R. J., Webb, A. J., Correia, C. S. C., Deutscher, N. M., Domingues, L. G., Feist, D. G., Gatti, L. V. J. A. C., and Physics: Consistent regional fluxes of CH4 and CO2 inferred from GOSAT proxy XCH4 : XCO2 retrievals, 2010-2014, Atmos. Chem.Phys., 17, 4781–4797, https://doi.org/10.5194/acp-17-4781-2017, 2017.

Guanter, L., Irakulis-Loitxate, I., Gorrono, J., Sanchez-Garcia, E., Cusworth, D. H., Varon, D. J., Cogliati, S., and Colombo, R.: Mapping methane point emissions with the PRISMA spaceborne imaging spectrometer, Remote. Sens. Environ., 265, 112 671, https://doi.org/10.1016/j.rse.2021.112671, 2021.

Hersbach, H., Bell, B., Berrisford, P., Hirahara, S., Horanyi, A., Munoz-Sabater, J., Nicolas, J., Peubey, C., Radu, R., Schepers, D., Simmons, A., Soci, C., Abdalla, S., Abellan, X., Balsamo, G., Bechtold, P., Biavati, G., Bidlot, J., Bonavita, M., De Chiara, G., Dahlgren, P., Dee, D., Diamantakis, M., Dragani, R., Flemming, J., Forbes, R., Fuentes, M., Geer, A., Haimberger, L., Healy, S., Hogan, R. J., Holm, E., Janiskova, M., Keeley, S., Laloyaux, P., Lopez, P., Lupu, C., Radnoti, G., de Rosnay, P., Rozum, I., Vamborg, F., Villaume, S., and Thepaut, J. N.: The ERA5 global reanalysis, Quarterly Journal Of the Royal Meteorological Society, 146, 1999-2049, 10.1002/qj.3803, 2020.

Iwaszenko, S., Kalisz, P., Slota, M., and Rudzki, A.: Detection of Natural Gas Leakages Using a Laser-Based Methane Sensor and UAV, Remote.Sens-Basel., 13, 510, https://doi.org/10.3390/rs13030510, 2021.

Krings, T., Neininger, B., Gerilowski, K., Krautwurst, S., Buchwitz, M., Burrows, J. P., Lindem ann, C., Ruhtz, T., Schuttemeyer, D., and Bovensmann, H.: Airborne remote sensing and in situ measurements of atmospheric CO2 to quantify point source emissions, Atmos.Meas. Tech., 11, 721–739, https://doi.org/10.5194/amt-11-721-2018, 2018.

Kuhlmann, R. and Buskens, C.: A primal-dual augmented Lagrangian penalty-interior-point filter line search algorithm, Math. Method.Oper. Res., 87, 451–483, https://doi.org/10.1007/s00186-017-0625-x, 2018.

Liu, D. and Michalski, K. A.: Comparative study of bio-inspired optimization algorithms and their application to dielectric function fitting, J.Electromagnet.Wave.,30, 1885–1894, https://doi.org/10.1080/09205071.2016.1219277, 2016.

Liu, F., Duncan, B. N., Krotkov, N. A., Lamsal, L. N., Beirle, S., Griffin, D., McLinden, C. A., Goldberg, D. L., and Lu, Z. F.: A methodology to constrain carbon dioxide emissions from coal-fired power plants using satellite observations of co-emitted nitrogen dioxide, Atmos.Chem. Phys., 20, 99–116, https://doi.org/10.5194/acp-20-99-2020, 2020.12.

Ma, D. and Zhang, Z.: Contaminant dispersion prediction and source estimation with integrated Gaussian-machine learning network model for point source emission in atmosphere, J. Hazard. Mater., 311, 237–245, https://doi.org/10.1016/j.jhazmat.2016.03.022, 2016.

Mays, K. L., Shepson, P. B., Stirm, B. H., Karion, A., Sweeney, C., and Gurney, K. R.: Aircraft-Based Measurements of the Carbon Footprint of Indianapolis, Environ. Sci. Technol., 43, 7816–7823, https://doi.org/10.1021/es901326b, 2009.

Nassar, R., Mastrogiacomo, J. P., Bateman-Hemphill, W., McCracken, C., MacDonald, C. G., Hill, T., O'Dell, C. W., Kiel, M., and Crisp, D.: Advances in quantifying power plant CO2 emissions with OCO-2, Remote. Sens. Environ., 264, 112 579, https://doi.org/10.1016/j.rse.2021.112579, 2021.

Nathan, B. J., Golston, L. M., O'Brien, A. S., Ross, K., Harrison, W. A., Tao, L., Lary, D. J., Johnson, D. R., Covington, A. N., Clark, N. N., and Zondlo, M. A.: Near-Field Characterization of Methane Emission Variability from a Compressor Station Using a Model Aircraft, Environ. Sci. Technol.,49, 7896–7903, https://doi.org/10.1021/acs.est.5b00705, 2015.

Pan, G., Xu, Y., and Huang, B.: Evaluating national and subnational CO2 mitigation goals in China's thirteenth five-year plan from satellite observations, Environ. Int., 156, 106 771, https://doi.org/10.1016/j.envint.2021.106771, 2021.

Robertson, A. M., Edie, R., Snare, D., Soltis, J., Field, R. A., Burkhart, M. D., Bell, C. S., Zimmerle, D., and Murphy, S. M.: Variation in Methane Emission Rates from Well Pads in Four Oil and Gas Basins with Contrasting Production Volumes and Compositions, Environ. Sci.Technol., 51, 8832–8840, https://doi.org/10.1021/acs.est.7b00571, 2017.

Schneising, O., Buchwitz, M., Reuter, M., Vanselow, S., Bovensmann, H., and Burrows, J. P.: Remote sensing of methane leakage from natural gas and petroleum systems revisited, Atmos. Chem. Phys., 20, 9169–9182, https://doi.org/10.5194/acp-20-9169-2020, 2020.

Shah, A., Pitt, J. R., Ricketts, H., Leen, J. B., and Allen, G.: Testing the near-field Gaussian plume inversion flux quantification technique using unmanned aerial vehicle sampling, Atmos. Meas. Tech., 13, 1467–1484, https://doi.org/10.5194/amt-13-1467-2020, 2020.

Shi, T., Han, G., Ma, X., Zhang, M., Pei, Z., Xu, H., Qiu, R., Zhang, H., and Gong, W.: An inversion method for estimating strong point carbon dioxide emissions using a differential absorption Lidar, J. Clean. Prod., 271, 122 434, https://doi.org/10.1016/j.jclepro.2020.122434,2020a.

Shi, T. Q., Ma, X., Han, G., Xu, H., Qiu, R. N., He, B., and Gong, W.: Measurement of CO2 rectifier effect during summer and winter using ground-based differential absorption LiDAR, Atmos. Environ.,

https://doi.org/10.5194/acp-2022-180
Preprint. Discussion started: 7 June 2022

Atmospheric Chemistry and Physics Discussions

220, 117 097, https://doi.org/10.1016/j.atmosenv.2019.117097, 2020b.

Tu, Q. S., Hase, F., Schneider, M., Garcia, O., Blumenstock, T., Borsdorff, T., Frey, M., Khosrawi, F., Lorente, A., Alberti, C., Bustos, J. J., Butz, A., Carreno, V., Cuevas, E., Curcoll, R., Diekmann, C. J., Dubravica, D., Ertl, B., Estruch, C., Leon-Luis, S. F., Marrero, C., Morgui, J. A., Ramos, R., Scharun, C., Schneider, C., Sepulveda, E., Toledano, C., and Torres, C.: Quantification of CH4 emissions from waste disposal sites near the city of Madrid using ground- and space-based observations of COCCON, TROPOMI and IASI, Atmos. Chem. Phys., 22, 295–317, https://doi.org/10.5194/acp-22-295-2022, 2022.

Varon, D. J., Jacob, D. J., Jervis, D., and McKeever, J.: Quantifying Time-Averaged Methane Emissions from Individual Coal Mine Vents with GHGSat-D Satellite Observations, Environ. Sci. Technol., 54, 10 246–10 253, https://doi.org/10.1021/acs.est.0c01213, 2020.

Varon, D. J., McKeever, J., Jervis, D., Maasakkers, J. D., Pandey, S., Houweling, S., Aben, I., Scarpelli, T., and Jacob, D. J.: Satellite Discovery of Anomalously Large Methane Point Sources From Oil/Gas Production, Geophys. Res. Lett., 46, 13 507–13 516, https://doi.org/10.1029/2019GL083798, 2019.

Venkatram, A.: An examination of the Pasquill-Gifford-Turner dispersion scheme, Atmos. Environ., 30, 1283-1290, https://doi.org/10.1016/1352-2310(95)00367-3, 1996.

Wolff, S., Ehret, G., Kiemle, C., Amediek, A., Quatrevalet, M., Wirth, M., and Fix, A.: Determination of the emission rates of CO2 point sources with airborne lidar, Atmos. Meas. Tech., 14, 2717–2736, https://doi.org/10.5194/amt-14-2717-2021, 2021.

Yuan, Q. and Qian, F.: A hybrid genetic algorithm for twice continuously differentiable NLP problems, Comput. Chem. Eng., 34, 36–41, https://doi.org/10.1016/j.compchemeng.2009.09.006, 2010.

Zhang, Y., Gautam, R., Pandey, S., Omara, M., Maasakkers, J. D., Sadavarte, P., Lyon, D., Nesser, H., Sulprizio, M. P., Varon, D. J., Zhang, R., Houweling, S., Zavala-Araiza, D., Alvarez, R. A., Lorente, A., Hamburg, S. P., Aben, I., and Jacob, D. J.: Quantifying methane emissions from the largest oil-producing basin in the United States from space, Sci. Adv., 6, eaaz5120, https://doi.10.1126/sciadv.aaz5120.

Zheng, B., Chevallier, F., Ciais, P., Broquet, G., Wang, Y., Lian, J., and Zhao, Y.: Observing carbon dioxide emissions over China's cities and industrial areas with the Orbiting Carbon Observatory-2, Atmos. Chem. Phys., 20, 8501–8510, https://doi.org/10.5194/acp-20-8501-2020,2020.

Zhou, X. C., Yoon, S. J., Mara, S., Falk, M., Kuwayama, T., Tran, T., Cheadle, L., Nyarady, J., Croes, B., Scheehle, E., Herner, J. D., and Vijayan, A.: Mobile sampling of methane emissions from natural gas well pads in California, Atmos. Environ., 244, 117 930, https://doi.org/10.1016/j.atmosenv.2020.117930, 2021.